Available online at www.sciencedirect.com
ScienceDirect
Polymer 48 (2007) 5388–5397
polymer
www.elsevier.com/locate/polymer

New insights into the characteristics of early stage crystallization of a polyethylene

Zhicheng Xiao, Yvonne A. Akpalu*

Department of Chemistry and Chemical Biology, Rensselaer Polytechnic Institute, Troy, NY 12180, USA

Received 9 May 2007; received in revised form 13 June 2007; accepted 16 June 2007
Available online 28 June 2007

Abstract

Small angle light scattering has been used to probe structure formation during isothermal crystallization of an ethylene-1-hexene copolymer (EH064, $M_w = 70{,}000$ g/mol, $\rho = 0.900$ g/cm^3, $M_w/M_n \sim 2$, 6.4 mol% hexene). It is shown that clear structural information on size scales ranging from hundreds of nanometers to several micrometers during early stage crystallization can be obtained by this method when crystallizing the polyethylenes at the high temperatures (above the peak melting temperature of a rapidly crystallized polymer sample) required for resolving early stage crystallization without the influence of the crystal growth. The results show that the early stage crystallization is characterized by large scale orientation fluctuations that precede the formation of local crystalline order manifest in X-ray scattering and the initial collapse of these large scale anisotropic/ordered domains. The scattering intensity increases exponentially with time initially, and the wave vector dependence of the growth rate of fluctuations is consistent with predictions for initial stages of a phase transformation process. However, the detailed mechanism cannot be described by existing models. The implications of our results are discussed within the context of proposed models for early stage crystallization.

Keywords: Crystallization; Polyethylene; Pre-ordering

1. Introduction

Polymer crystallization is an industrially and scientifically important phenomenon that has eluded detailed molecular description. The chemical structure of the polymeric chain, combined with morphological features acquired during processing, governs the properties of semicrystalline polymers. Investigations of the details of liquid–solid transformation have closely paralleled the development of polymer science, and interest in understanding the details of crystalline structure has arisen from the well known fact that the crystallinity controls the properties of the material. Polymer crystallization is believed to follow the classical nucleation and growth theory of the crystal nuclei into a hierarchy of ordered structures, which involves the growth of lamellar crystals and the aggregation of these lamellae into superstructures, such as spherulites and axialites [1–3]. The primary lamellar habit formed is a consequence of the anisotropic growth of crystal nuclei. However, the fundamental mechanisms of polymer crystallization, especially at the early stage, are still poorly understood [4–8]. While considerable theory [5–13] of crystallization kinetics has been developed, there is concern as to whether the predicted mechanisms are unique.

For many years, nucleation and growth as a stepwise process has dominated the discussion of polymer crystallization [1,6]. In contrast to this view, Olmsted et al. [11,14,15] proposed a theory, based on spinodal decomposition of a melt, to explain the observations of peak in SAXS experiments before the emergence of crystalline structure [14–21]. On the other hand, Strobl [8,12] proposed a multistage process to explain polymer crystallization, which concludes that a mesomorphic melt formed as precursor of crystallization. Common to both views is that the crystallization is preceded by an ordered precursor (so-called pre-ordering). However, clear

* Corresponding author.
E-mail address: akpaly@rpi.edu (Y.A. Akpalu).

0032-3861/$ - see front matter © 2007 Elsevier Ltd. All rights reserved.
doi:10.1016/j.polymer.2007.06.049

structural information about such possible precursors – necessary to verify these hypotheses – is still scarce. As a result, during recent years an important and still open debate has been going on regarding polymer crystallization. Interestingly, pre-ordering was already implied in some rather early studies of polymer crystallization, but it did not receive much attention. As early as 1967 Katayama et al. [22,23] observed a small angle X-ray scattering (SAXS) peak significantly earlier than the appearance of the corresponding crystalline Bragg peaks in wide angle X-ray scattering (WAXS). They proposed that density fluctuations occurred before the formation of any crystals. The idea of a multistage process dates back to 1967 in a study by Yeh and Geil [24], while in 1981 Schultz introduced a spinodal approach promoting orientation in polymer systems [25]. Lindenmeyer suggested the idea that polymer crystals grow by accretion of ''prefolded'' chains 30 year ago [26], and shortly after that, Allegra [27] proposed a detailed ''bundle theory'' for polymer crystallization of metastable, prefolded chains. However, the essential question about the nature of pre-ordering still remained open. The description 'pre-ordering before crystallization' is often not used in a precise way. In spite of this, it is evident that the precursor should possess some ordering intermediate between the liquid and the crystal phase.

To verify the mechanisms proposed, many experimental efforts [14,20,28–37] have been conducted. Simultaneous SAXS and WAXS experiments with synchrotron source are powerful tools to investigate the kinetics and morphological features during crystallizations of various polymer systems under different conditions [14–16,28,29,33,38–42]. Conflicting results favoring various proposed models have been reported. Imai et al. [16,17], Ezquerra et al. [18] and Terrill et al. [19] reported the observations of SAXS peak preceding the development of the crystalline peaks in WAXS region for poly(ethylene-terephthalate) (PET), polyetheretherketone (PEEK) and polypropylene (PP), respectively. Others [28,40,42] reported that no such preceding peak in SAXS before WAXS can be observed for polyethylene (PE) and some other polymers. The possibility that the observations may be due to the detection limit of X-rays which has been discussed [14,40]. Atomic force microscopy (AFM) [32,34,43] has also been used to investigate the structural evolution during polymer crystallization, and recent studies [34] on a branched polyethylene (3.8 mol% butene) shows that large scale structures (1–3 μm) are formed before the formation of any local crystalline structure. The evolution of these large scale structures during early stage crystallization is still unclear. Other techniques including differential scanning calorimetry (DSC) [34], small angle neutron scattering (SANS) [36], etc., have also been used to probe the structure changes during early stage crystallization, but until present, strong proof or disproof for any of the models has been scarce. Also, computer simulation has been employed to elucidate the possible mechanisms for early stage crystallization [44–52]. Early stage crystallization behaviors of single chain [44], multiple chains [44,47,50–52], in melt [48,51] or in solution [45,46] have been examined by various simulation methods, but no convincing conclusion has been reached. It has been suggested that growth rate (Ω_q) of scattering intensities during early stage crystallization is a good criterion for distinguishing the proposed mechanisms [7,15,47,50,51,53], since different models predict different behavior for Ω_q/q^2 versus q^2. Ryan et al. [14,15,53] used Cahn–Hilliard analysis to fit the SAXS data obtained before the emergence of WAXS peak in the framework of spinodal decomposition model, and the ''spinodal temperatures'' have been estimated. Muthukumar [50] has argued that, if the mechanism for early stage crystallization is simply spinodal decomposition, the Ω_q/q^2 versus q^2 plots should show a monotonic linear decrease from a finite positive value at $q \to 0$ with a slope independent of quench depth, which is not experimentally observed.

To investigate the structural changes and evolution of fluctuations during early stage crystallization of polyethylenes, high crystallization temperatures are required. We have previously [54] shown that SALS under cross-polarized (H_V) alignment and USAXS can be used to probe structural changes during early stage crystallization of polymers by crystallizing the polyethylene sample at temperatures higher than the peak melting temperature. Our results showed that during early stage crystallization of polyethylene–olefin copolymers, large scale (>1 μm) fractal domains with diffuse interfaces are formed initially, and the interfaces of these domains sharpen with time. In this paper, the nature of the fluctuations during early stage crystallization is presented and discussed in the context of the various proposed models.

2. Materials and methods

2.1. Sample preparation

The ethylene–1-hexene copolymer (EH064, $M_w =$ 70,000 g/mol, $\rho = 0.900$ g/cm^3, $M_w/M_n \sim 2$, 6.4 mol% hexene) studied was provided by ExxonMobil. The peak melting temperature (T_m^p) and the final melting temperature (T_m^f) of the rapidly crystallized EH064 sample are 95 °C and 103 °C, respectively. The copolymer was prepared with a metallocene catalyst. Before any further sample preparation, 3 g of polymer was dissolved in 300 mL of refluxing toluene at 111 °C. The solution was poured into an acetone/methanol (50/50) mixture (800 mL) at 0 °C. The resulting precipitate was filtered, washed, and dried under vacuum at 40–50 °C for 72 h [55].

2.2. Simultaneous WAXS and SAXS

Samples were melt-pressed in a vacuum laboratory hot press (Carver Press, Model C) at 160 °C for 30 min. The molded films were then allowed to cool to room temperature under vacuum. A dual temperature chamber for the melt crystallization experiments consists of two large thermal chambers maintained at the melt temperature ($T_1 = 160$ °C) and the crystallization temperature ($T_2 = 81$ °C, 83 °C, 86 °C, 89 °C, 92 °C or 96 °C). After 5–10 min at T_1, the copper sample cell was transferred rapidly (~2 s) to the other chamber by

means of a metal rod connected to a pneumatic device. A detailed description of the arrangement of the sample and of the two detectors used to measure WAXS and SAXS simultaneously has been provided previously [39]. Each polymer sample within the copper cell was 1.5 mm thick and 7 mm in diameter and was contained between two 25 μm thick Kapton films. The actual sample temperature during crystallization (T_2) and melting (T_1) was monitored by means of a thermocouple inserted into the sample cell. The crystallization temperature was usually reached 120 s after transfer without overshooting. Under isothermal conditions the fluctuations in the sample temperature are less than 0.5 °C. The references to time are times elapsed after transferring the sample to the crystallization chamber. Simultaneous WAXS and SAXS experiments on some samples which were first maintained at $T_1 = 180$ °C instead of 160 °C were also performed, and no difference was observed for both the time evolution of invariant from SAXS and crystallinity determined from WAXS. In this paper, the simultaneously WAXS and SAXS data obtained for the samples first maintained at 160 °C are presented.

Time-resolved simultaneous SAXS/WAXS data were collected at the Advanced Polymer Beamline at Brookhaven National Laboratory, X27C. The radiation spectrum from the source was monochromated using a double multilayer monochromator and collimated with three 2° tapered tantalum pinholes to give an intense X-ray beam at $\lambda = 1.307$ Å. Two linear position sensitive detectors (European Molecular Biology Laboratory, EMBL) were used to collect the SAXS and WAXS data simultaneously. The usable span of scattering vector magnitudes ($q = (4\pi/\lambda)\sin(\theta/2)$, where λ is the X-ray wavelength and θ is the scattering angle) for SAXS, was in the range $0.01\ \text{Å}^{-1} < q < 0.3\ \text{Å}^{-1}$, while that for WAXS was $0.7\ \text{Å}^{-1} < q < 2.9\ \text{Å}^{-1}$. Data were collected in 15 s or 30 s time blocks, depending on the crystallization rate. The peak position, peak height and peak width for the crystalline and amorphous reflections in WAXS were extracted by a curve fitting program. A broad Gaussian peak was used to describe the amorphous background. The crystalline peaks (110 and 200) were also fitted with Gaussian functions. For SAXS, the scattering intensity due to thermal fluctuations was subtracted from the SAXS profile $I(q)$ by evaluating the slope of $I(q)q^4$ versus q^4 plots [56] at large wave vectors ($q \gg 0.2\ \text{Å}^{-1}$).

2.3. Small angle light scattering (SALS)

SALS measurements were performed on (90–200 μm thick) film samples sealed between two round glass coverslips. Before the measurements, the sealed samples were heated from room temperature to 180 °C, held at this temperature for 5 min, and then quenched to the crystallization temperature (T_c). After reaching T_c, the samples were immediately heated to 180 °C, held at this temperature for 10 min and then cooled to T_c for measurements. The heating/cooling rate used was about 50 °C/min. An Instec HCS600V hot stage was used to control the temperature within 0.1 °C during crystallization measurements. SALS patterns under cross-polarized (H_V) and parallel-polarized (V_V) optical alignments and transmitted light were recorded using a vertical light scattering apparatus described previously [57]. For this work, the usable span of scattering vector magnitudes was in the range $0.2\ \mu\text{m}^{-1} < q < 2.4\ \mu\text{m}^{-1}$. A mirror attached to the center of the screen was used to reflect the light transmitted by the sample and the intensity of this light was measured by means of a computer controlled optical power meter. All measurements were performed under nitrogen atmosphere.

Experimental scattering intensities from SALS were corrected using procedures previously described [57]. The melt contribution to the corrected H_V scattering intensity was subtracted after accounting for statistical fluctuations. The percent transmission was determined from the ratio of the transmitted light intensity measured with a sample in the beam path to that measured without the sample.

Crystallization mechanisms can be determined by comparing the time evolution of degree of crystallinity and the total integrated scattering intensity or invariant [28,38]. In this paper, we calculated the degree of crystallinity from WAXS (w_c) and the total integrated scattering intensities or invariant from SAXS (Q_{SAXS}) and H_V SALS (Q_{H_v}). The degree of crystallinity is obtained by using the methods previously described [28]. The uncertainty in w_c by this method is about 2%.

The SAXS invariant (Q_{SAXS}) or H_V SALS invariant (Q_{H_v}) determined from measurements represents fluctuations in the sample and will be referred to as relative invariants.

$$Q_{SAXS} \propto \langle \eta^2 \rangle$$

$$Q_{H_v} \propto \langle \delta^2 \rangle$$

where $\langle \eta^2 \rangle$ represents the nanoscale mean-square density fluctuations of the system, $\langle \delta^2 \rangle$ represents the micro-scale mean-square fluctuations in the averaged anisotropy of the system.

3. Results

When a crystallizable polymer is cooled below its equilibrium melting temperature, the hierarchical structure formed can be probed by in situ scattering. Light scattering is sensitive to the objects with sizes larger than several hundred nanometers whereas the X-rays are sensitive to nanoscale structures. The crystallization process can be described by two stages: (1) primary crystallization with the growth of superstructures, and (2) secondary crystallization during which the degree of crystallinity within the morphological units increases. These crystallization mechanisms can be determined by comparing the time evolution of the degree of crystallinity (w_c) determined from WAXS and the total integrated scattering intensity or invariant during crystallization from SAXS [28,38].

Fig. 1 shows WAXS, SAXS and SALS results during isothermal crystallization of EH064. When EH064 is crystallized at temperatures lower than $T_m^p = 95$ °C, primary crystallization is rapid. At $T_c = 90$ °C, the percent transmission (Fig. 1(c)) reaches a constant value after going through a minimum within 4 min, indicating that the spherulites become space-

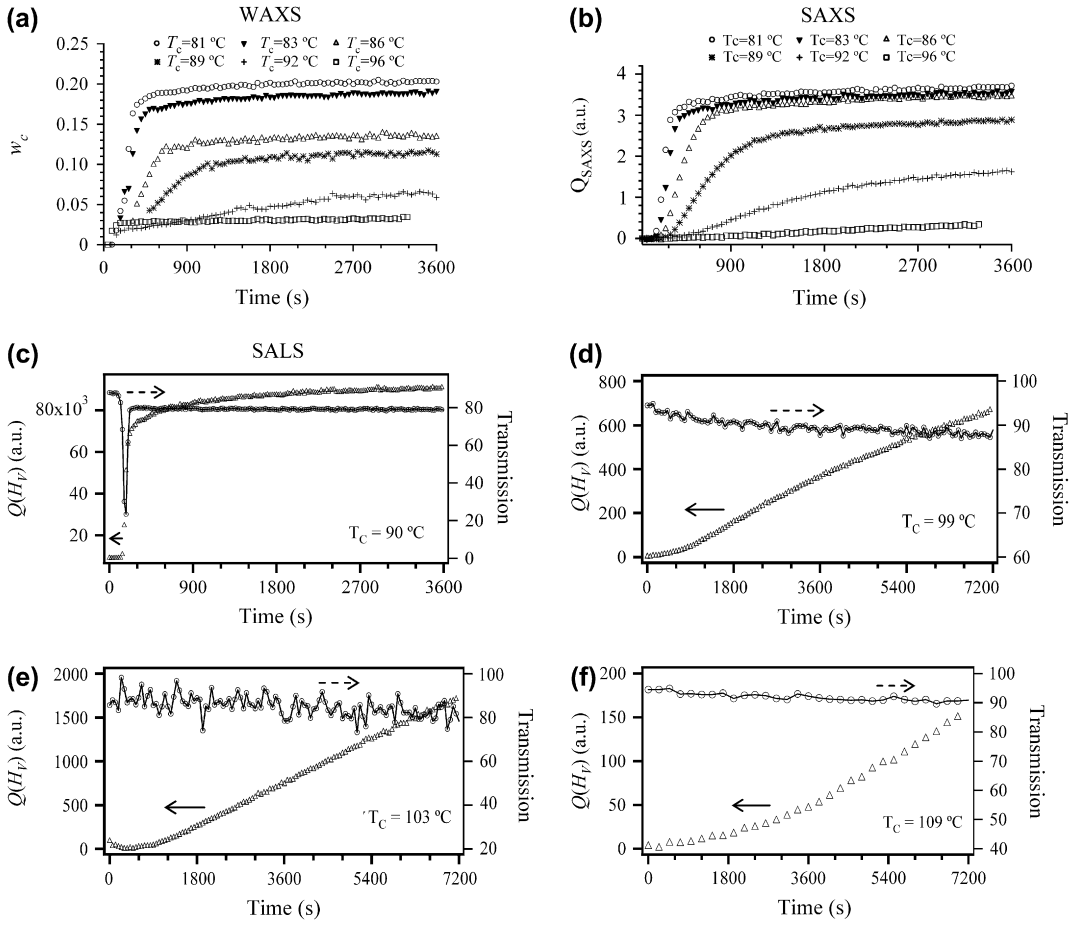

Fig. 1. Crystallization behavior of EH064 from (a) wide angle X-ray scattering (WAXS), (b) small angle X-ray scattering (SAXS) at various crystallization temperatures and (c) small angle light scattering (SALS) at 90 °C, (d) at 99 °C, (e) at 103 °C and (f) at 109 °C. The time evolutions of WAXS crystallinity (w_c) and SAXS invariant (Q_{SAXS}) are shown. For light scattering, H_V SALS invariant (Q_{H_V}) and percent transmission measured simultaneously with H_V SALS are shown.

filling at very early time [58]. During this period, the sharp increase in the H_V SALS invariant (Fig. 1(c)) is consistent with rapid growth of the spherulites. The slower increase in the H_V SALS invariant at longer times can be attributed to the dominance of secondary crystallization. Thus, the increase in the invariant from SAXS (Fig. 1(b)) and crystallinity from WAXS (Fig. 1(a)) at longer times can be attributed to the secondary crystallization. These results are consistent with what has been observed for other polyethylene [58] and polypropylene [31] samples during crystallization.

As the crystallization temperature is increased the crystallinity decreases. At temperatures near the peak melting temperature, it is difficult to resolve changes in the SAXS invariant and crystallinity determined from WAXS because crystallinity is small (<5%) and close to the detection limits. As the crystallization temperature is increased further, the very low crystallinity attainable and large thermal fluctuations make it difficult to detect the changes in crystallinity and structure by X-rays [28,40,59]. However, if large scale fluctuations are present during early stage crystallization, SALS can be used to investigate the structural changes at these temperatures [54].

Fig. 2 shows SALS patterns for EH064 from SALS at various temperatures and crystallization times. As expected, the typical anisotropic H_V and V_V patterns obtained at 90 °C indicate the formation of space-filling spherulites at crystallization temperatures below $T_m^p = 95$ °C. When samples are crystallized at temperatures above $T_m^p = 95$ °C, the initial H_V SALS patterns exhibit circular symmetry consistent with the formation of anisotropic domains that are randomly oriented with each other. Anisotropic four-leaf H_V patterns and corresponding isotropic V_V patterns were obtained for crystallizations at 99 °C and 103 °C, indicating the formation of non-space-filling spherulites or incomplete spherulites (axialites) at these temperatures [60]. At 99 °C, the maximum attainable crystallinity is about 3% and it is about 1% for 103 °C (Fig. 3, [61,62]). When the samples were crystallized at the temperatures higher than $T_m^f = 103$ °C (107 °C and 113 °C as shown in Fig. 2), isotropic patterns are observed for both H_V and V_V SALS scattering. At these temperatures, although the theoretical crystalline fraction of EH064 is less than 10^{-3} (Fig. 3, [61,62]), polarized light scattering due to the organization of crystals can be observed whereas the crystallinity cannot be directly measured by DSC or X-rays. Thus analysis of the SALS patterns can yield information regarding the nature of the anisotropic domains formed during the initial stages of crystallization.

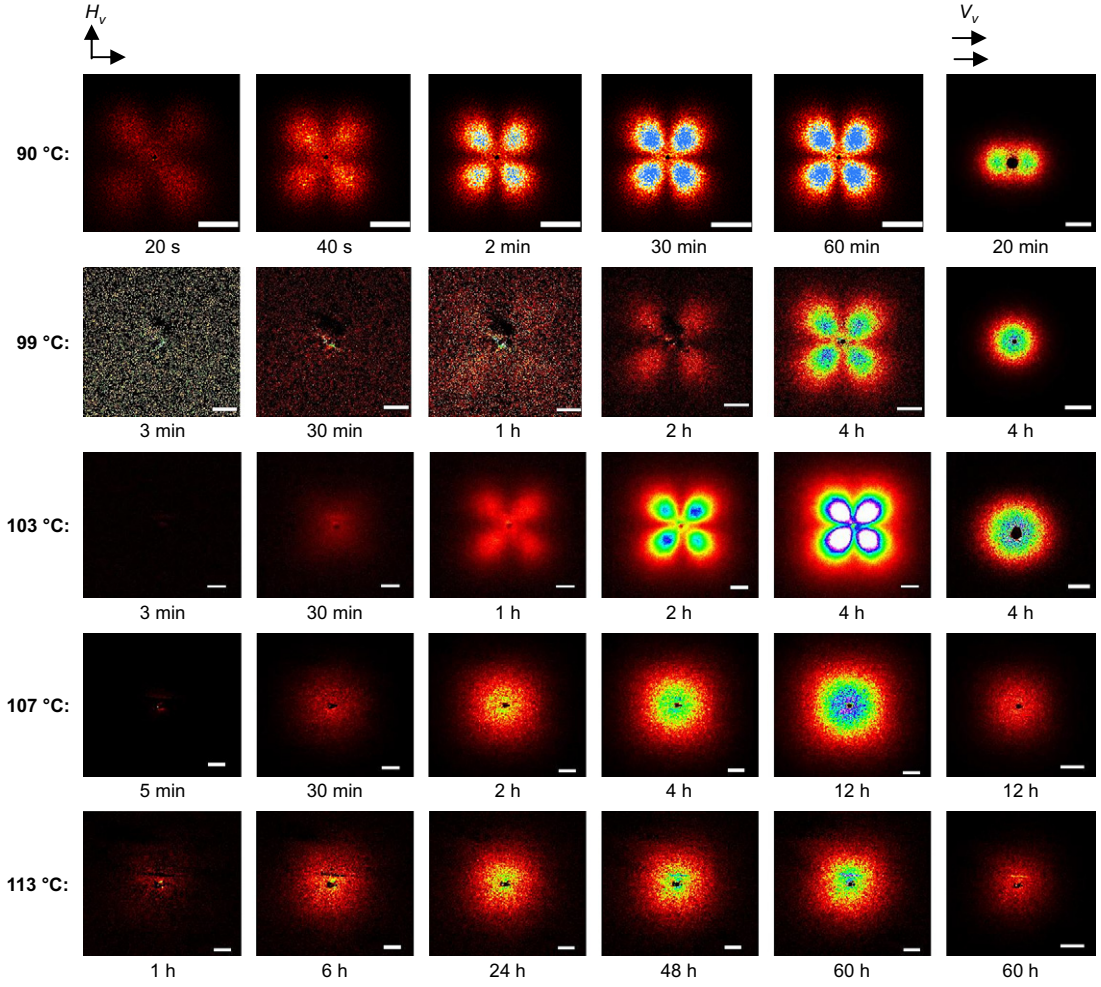

Fig. 2. H_V and V_V SALS patterns during isothermal crystallization of a polyethylene (EH064) at different crystallization temperatures. For all patterns, the scale bar is equal to a scattering angle of 5°. From DSC, the peak melting temperature (T_m^p) and final melting temperature (T_m^f) of the rapidly crystallized EH064 sample are $T_m^p = 95$ °C, $T_m^f = 103$ °C, respectively.

The circularly averaged intensity of the H_V SALS patterns at 113 °C monotonically decreases with scattering vector q (Fig. 4(a)). The increase in intensity with time can be associated with the increases in the number and/or the anisotropy of the domains. In Fig. 4(b), the shape of the log–log plots of scattering profiles indicates that the domains are fractal objects. Kratky plots have been used to examine the conformations of macromolecules [63], such as proteins [64] and RNAs [65]. In (Fig. 4(c)), the Kratky plots shown indicate that, initially, these domains are coil-like open structures. At longer times (>6 h), the domains become more compact as evident by the changes in the overall shape of the Kratky plots. The magnitude of limiting slope of log–log plots of SALS profiles increase with time also indicates the interfaces of these domains are sharpening with time. Our previous ultra-small-angle X-ray scattering (USAXS) measurements [54] during isothermal crystallization of EH064 at 99 °C also showed that fractal objects with sizes larger than 100 nm are formed during the initial stages. The magnitude of limiting slope of log–log plots of USAXS profiles increases with time, which is similar to the observation from SALS measurement (Fig. 4(b)). At the same time, no structure change is observed in the traditional SAXS region [54]. SALS experiments on crystallization of other polyethylenes (an ethylene–butene copolymer, EB059, $M_w = 70{,}000$ g/mol, $\rho = 0.900$ g/cm^3, $M_w/M_n \sim 2$, 5.9 mol% butene and linear polyethylene, $M_w = 32{,}100$ g/mol) at high temperatures also show similar scattering profiles due to large scale fractal objects [54].

Our results show that anisotropic large scale (size comparable to the wavelength of the light used, 633 nm) fractal domains are formed during early stage crystallization of the polyethylene studied. The average size of the domains formed can be obtained by performing Guinier analysis on the monotonically decreasing H_V SALS scattering profiles observed, and the Guinier analysis is given by the following equation,

$$I(q) = I(q \to 0)\exp\left[-\frac{R_g^2 q^2}{3}\right], \quad (1)$$

where R_g is the radius of gyration of these domains. The results for isothermal crystallization of EH064 at 107 °C and 113 °C are shown in Fig. 5. The results show good agreement with Eq (1) in low q region ($0.05\ \mu m^{-2} < q^2 < 0.4\ \mu m^{-2}$).

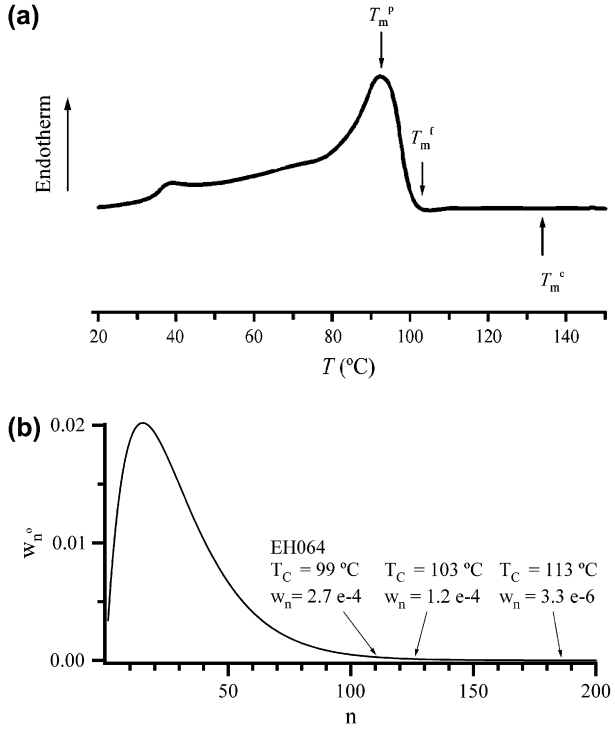

Fig. 3. (a) Typical differential scanning calorimetery (DSC) melting curve of EH064 sample rapidly crystallized from melt. Heating rate: 10 °C/min. (b) Overall distribution of *n*-sequences for random polyethylene–hexene copolymer [62]. The arrows indicate the critical length of ethylene sequences which is in equilibrium with undercooled melt at given temperatures, and the sum of all weight fractions for *n* greater than this value is the theoretical crystallinity for the corresponding temperatures.

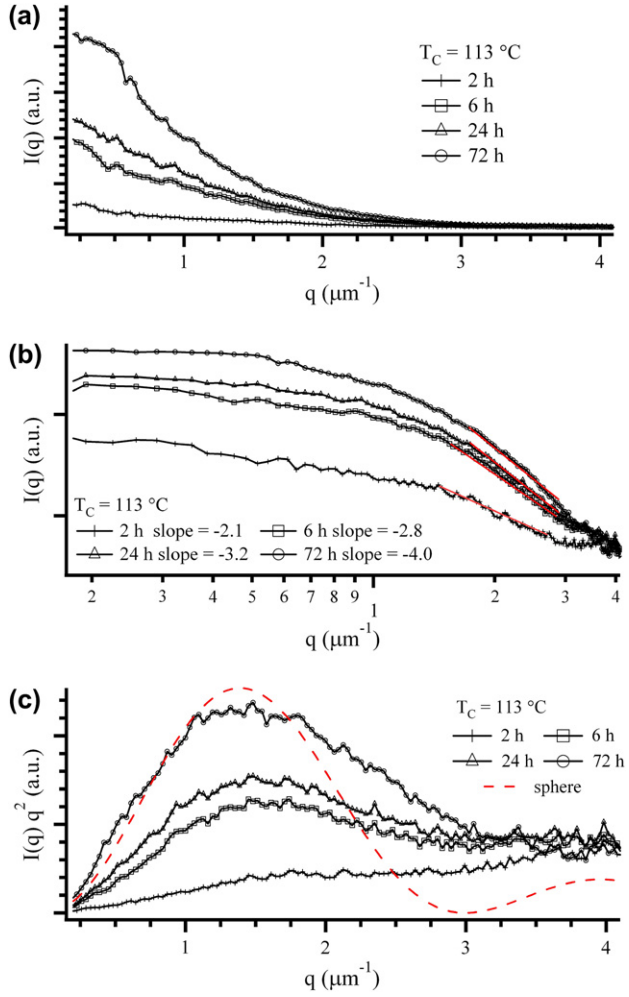

Fig. 4. (a) H_V SALS scattering profiles ($I(q)$ versus q) for isothermal crystallization of EH064 at 113 °C. (b) Log–log plot of H_V SALS scattering profiles for isothermal crystallization of EH064 at 113 °C. (c) Kratky plots (Iq^2 versus q) of H_V SALS scattering for isothermal crystallization of EH064 at 113 °C, dashed line represents a sphere with a diameter of 1.5 μm.

Similar results are obtained for crystallization at other temperatures ($T_c = 109$ °C and 111 °C). For all temperatures higher than the final melting temperature ($T_c = 107$ °C, 109 °C, 111 °C, and 113 °C), the R_g value decreases initially and then reaches to a relatively constant value (Fig. 6).

4. Discussion

Our results show that all stages of polymer crystallization can be studied by the combinational use of X-ray and light scattering. At temperatures below the peak melting temperature ($T_c < 95$ °C for EH064), the crystallization kinetics can be resolved by comparing the time evolution of degree of crystallinity determined from WAXS and the total integrated scattering intensity from SAXS [28,38]. As temperature is increased from $T_m^p = 95$ °C, crystallization is increasingly dominated by primary crystallization. During this process, the formation of the initial lamella crystals and subsequent crystal growth process can be probe by using real time SAXS measurements [28,40]. When the crystallization temperature is higher than $T_m^f = 103$ °C (107 °C and 113 °C shown in Fig. 2), the time variation of the degree of crystallinity from WAXS and invariant from SAXS is not useful for elucidating the crystallization mechanism because of the very small volume fraction of crystals involved [40]. From SALS (Fig. 2), the crystallization process at temperatures above $T_m^f = 103$ °C is characterized by the formation of large scale randomly oriented anisotropic domains before the formation of any local crystalline structure. Large scale structures during the early stages of crystallization have been observed by AFM [13,34]. Thus, this behavior is a characteristic of the initial stages of crystallization which we refer to as early stage crystallization.

Our results show that the large anisotropic domains (or precursors) observed during early stage crystallization contract initially, and then the size of these domains remains relatively constant while associated orientation fluctuations increases, indicating orientational ordering of the domains. Some recent simulation studies [44,66–68] have suggested that crystallization proceeds through a globally collapsed amorphous state, the entire amorphous chain become compact, and subsequently transform to the stable crystalline state with ordering in all parts of the system simultaneously. Our observation of the initial decreasing in the radius of gyration of the domains formed is consistent with this process (so-called "global collapse"). Thus it can be concluded that we do resolve early

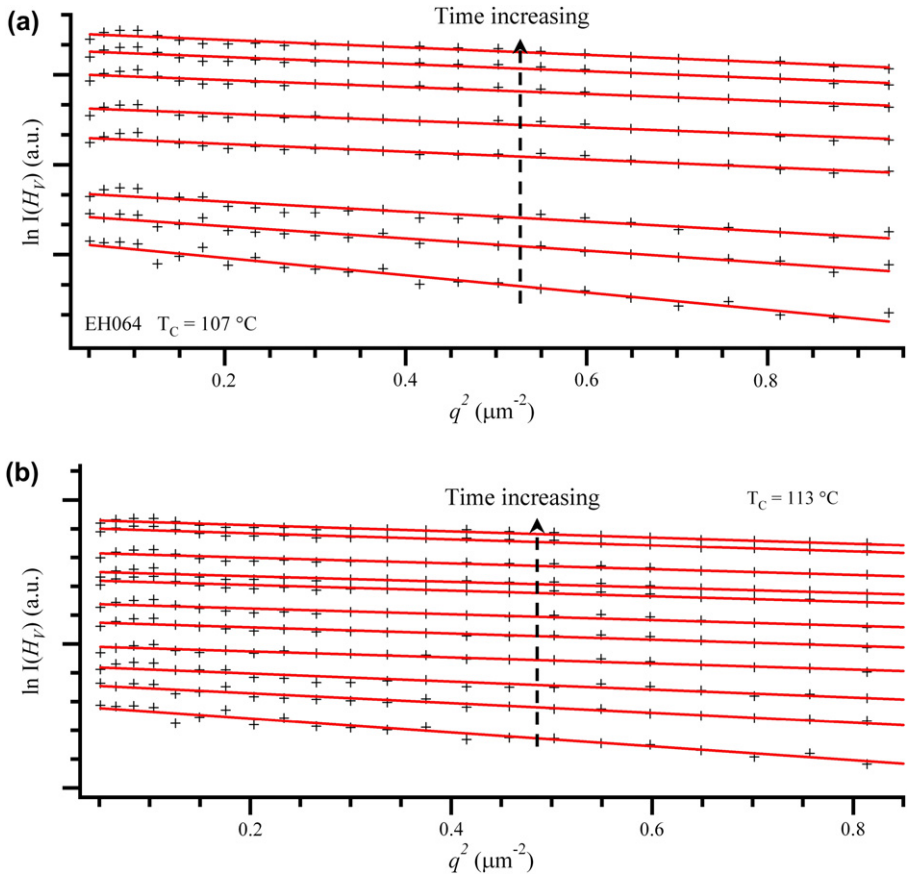

Fig. 5. Guinier analysis of SALS scattering profiles obtained during early stage crystallization of EH064 at (a) 107 °C and (b) 113 °C.

stage behavior at crystallization temperatures higher than $T_m^f = 103$ °C.

As detailed in the introduction, several theoretical models have been proposed for the densification process prior the formation of crystals, which include the spinodal-assisted nucleation model by Olmsted et al. [11] and the nucleation and growth model by Muthukumar [7]. The evolution of density fluctuation during early stage crystallization has been predicted by these models. The "spinodal-assisted" nucleation model for early stage crystallization of polymer predicts [11,14,15] that a metastable liquid–liquid (LL) phase coexistence curve lies buried inside the equilibrium liquid–crystal coexistence region, and the coupling between density and chain conformation induces a liquid–liquid binodal within the equilibrium liquid–crystalline solid coexistence region. Experimentally, Cahn–Hilliard [69] analysis for spinodal decomposition has been used to analyze the SAXS profiles obtained during the "induction period" (from the capture of the peaked profile in SAXS until the appearance of crystalline peak in WAXS region) by Ryan et al. [14,15]. Generally, for a binary fluid undergoing a demixing instability, fluctuations $\Psi(q)$ in composition grows exponentially, and the variation in scattering intensity, $I(q,t) = \langle \psi(q,t)\psi(-q,t)\rangle$, also grows exponentially is given by the following equation:

$$I(q,t) = I(q,0)\exp[2R(q)t]$$

$R(q)$, which is termed as the growth rate constant and it is given by

$$R(q) = -Mq^2\left[\frac{\partial^2 G}{\partial \rho^2} + 2\kappa q^2\right]$$

where M is the mobility term, G is Gibbs free energy, and κ is gradient free energy term.

Thus, the $R(q)/q^2$ term can be taken as a measure of dynamic driving force for the growth of the concentration fluctuation with wave vector $q/2\pi$. For the spinodal-assisted

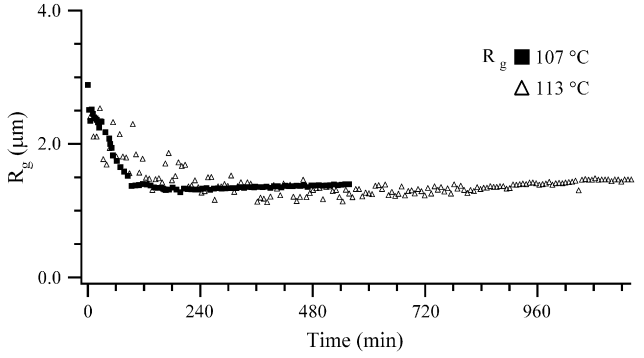

Fig. 6. Time dependence of radius of gyration (R_g) values for crystallization at 107 °C and 113 °C.

model, a plot of $R(q)/q^2$ versus q^2 is expected to be linear for a given region of q [14,15].

It has been argued by Muthukumar that, the polymer crystallization process is similar to the nucleation and growth in small molecular systems, except that for the polymer system, the polymer chain is long enough to participate in several nuclei. During the early stages of crystallization, several ''baby nuclei'' are formed by the same single polymer chain. The strands connecting these baby nuclei are flexible with considerable configurational entropy. As time progresses, the monomers in the flexible strands are reeled into the baby nuclei while the orientational order in each nucleus increases. And simultaneously, the competition between nuclei for further growth dissolves some nuclei. As a result, a folded-chain structure emerges. The average distance between baby nuclei does not change with time in the initial times. Furthermore, Muthukumar proposed that [47] the free energy of a system with ''baby nuclei'' connected by strands comes from the following three terms: (1) density difference ψ between the ''baby nuclei'' and the amorphous background giving a free energy contribution that is proportional to $-\Delta T\psi^2(\Delta T = T_m^0 - T)$; (2) interfacial free energy given by the square gradient of ψ, proportional to $q^2\psi_q^2$ (where q is the scattering wave vector); and (3) monomer–monomer correlation arising from the chain connectivity of the connector participating in multiple nuclei, leading to a free energy contribution that is proportional to $q^{-2}\psi_q^2$ (as in the Debye structure factor for length scales shorter than R_g). Thus, it goes as

$$F \sim \sum_q \left(-\Delta T + q^2 + q^{-2}\right)\psi_q^2;$$

where all the prefactors are left out. For the early stages of nucleation and growth, ψ evolves with time, in accordance with the relaxation of the chemical potential gradient, as we see here:

$$\frac{\partial\psi(r,t)}{\partial t} \approx -\nabla\left(-\nabla\frac{\partial F}{\partial T}\right), \text{ so that}$$

$$\frac{\partial\psi_q(t)}{\partial t} = -q^2\left(-\Delta T + q^2 + \frac{1}{q^2}\right)\psi_q(t).$$

Thus, the scattering intensity, $I(q,t)$, proportional to $\langle\psi_q^2(t)\rangle$, is expected to be exponential with time, $I(q,t) \sim \exp(2\Omega_q t)$, with the rate $\Omega_q = q^2(-\Delta T + q^2 + q^{-2})$. Then, $\Omega(q)/q^2$ is expected to rise sharply with q^2, and to reach a maximum and then decrease at higher q values according to Muthukumar's model. This behavior is distinct from a spinodal-assisted mechanism where $\Omega(q)/q^2(R(q)/q^2)$ is expected to vary linearly with q^2.

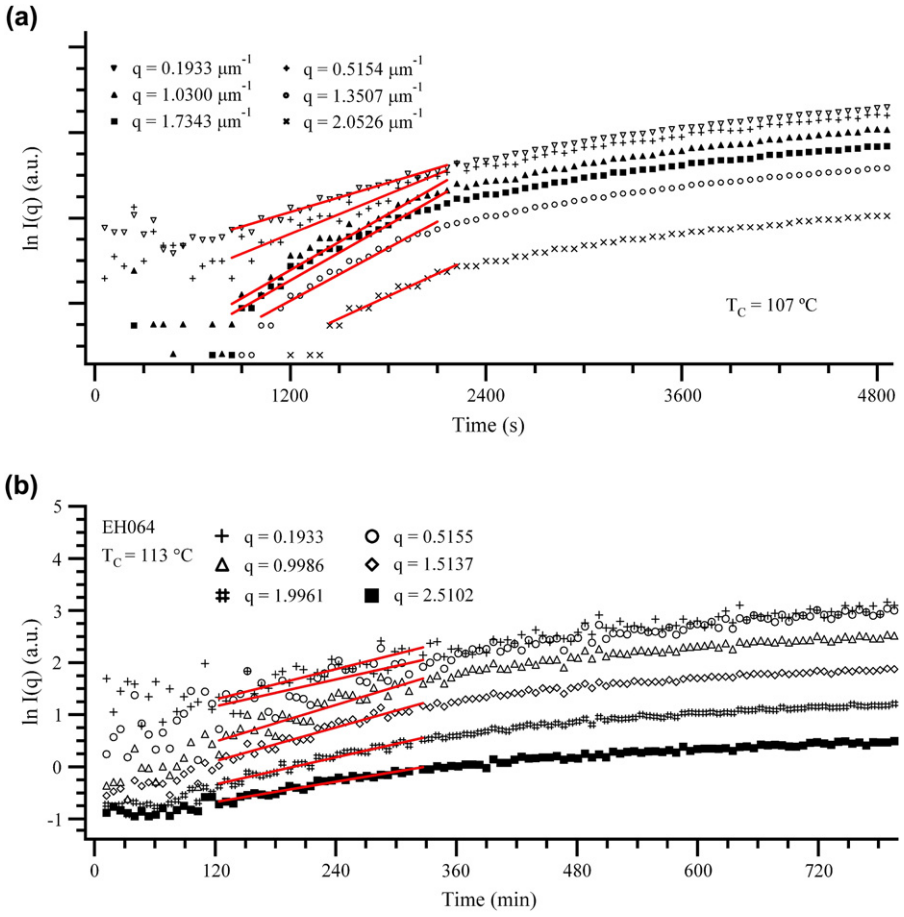

Fig. 7. Growth rate of the scattering intensity at various q values during crystallization of EH064 at (a) 107 °C and (b) 113 °C.

For early stages of a phase transition process, the fluctuations/intensities are predicted to be increased with time exponentially for any proposed models. To facilitate the comparison of our results with the theoretical models for early stage crystallization, the growth rates of scattering intensity (Ω_q) at various q values are evaluated from the slope of $\ln I$ versus time plots (Fig. 7) since the intensities exponentially increase with time during initial times. Growth rate (Ω_q) versus q profile expected for initial stages of a phase transition process is obtained for crystallization at 113 °C, and the deviation of growth rate (Ω_q) versus q profile observed (Fig. 8) for crystallization at 107 °C indicates that there still might be some effect from crystal growth process present at this temperature. At 113 °C, the growth rate reaches a peak value in mediate q values, and it is relatively smaller in low q and high q region. It has been reported that the Ω_q/q^2 decreases with q^2 linearly at given q region from the analysis of SAXS profiles obtained during early stage crystallization of PET [17], iPP [19,53] and PEEK [18] as evidence of the presence of spinodal decomposition during early stage crystallization. Our analysis (Fig. 9) shows no linearity on Ω_q/q^2 versus q^2 plots. The results show that Ω_q/q^2 value decreases sharply with q^2 at low q region and is relatively constant at medium and high q region.

It must be noted that we have obtained similar SALS scattering profiles for crystallization of linear polyethylene and other branched polyethylenes (ethylene–1-butene copolymers) [54], indicating that this densification process observed is a universal process for polyethylenes. For EH064 used in this study, ethylene sequences with less than 185 carbons are not crystallizable at 113 °C as indicated by Fig. 3 [62]. At these high crystallization temperatures, since only a very small portion of long ethylene sequences can crystallize (maximum attainable crystallinity at 113 °C is less than 10^{-4} [62]), it is unlikely that the chain length distribution of crystallizable species will influence the crystallization behavior. Our results clearly show that early stage crystallization is characterized by large scale orientation fluctuations that precede the formation of local crystalline order. A second characteristic is the initial "global collapse" of these large scale anisotropic/ordered domains. Although these observations are consistent with the predictions of current theoretical models [7,8,11,68] and simulations [44,66,67], new models are required to correctly predict the spatial dependence and time evolution of these orientation fluctuations characteristic of the initial stages of polymer crystallization from the melt state.

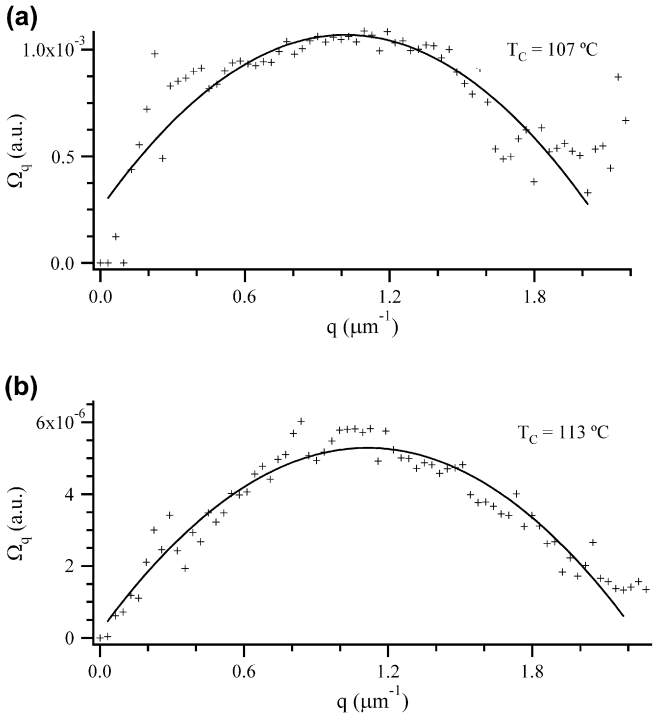

Fig. 8. Dependence of growth rate (Ω_q) of the scattering intensity on scattering vector q for crystallization of EH064 at (a) 107 °C and (b) 113 °C.

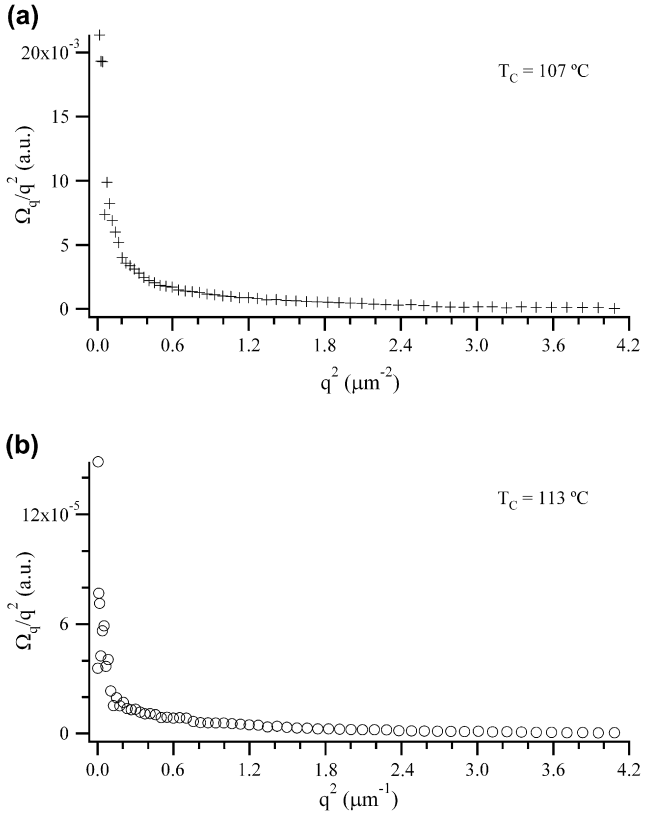

Fig. 9. Dependence of Ω_q/q^2 on q^2 for crystallization of EH064 at (a) 107 °C and (b) 113 °C.

Acknowledgements

We would like to acknowledge support of this work by NSF CMMI under Award # 0600317. The SALS instrument used for this work was developed with National Science Foundation support under NSF DMR-0108976. Simultaneous SAXS and WAXS experiments were carried out by Y.A.A. at Beamline X27C of National Synchrotron Light Source, Brookhaven National Laboratory, which is supported by Department of Energy, Division of Materials Sciences and Chemical Sciences.

Y.A.A. would like to thank NIST for support of the use of beamline X27C. We would also thank Dr. D.J. Lohse (Exxon-Mobil) for providing the copolymers. Additionally, we would like to thank B. Crist for helpful discussions.

References

[1] Lauritzen JI, Hoffman JD. Journal of Research of the National Bureau of Standards Section A Physics and Chemistry 1960;64:73–102.
[2] Hoffman JD, Lauritzen JI. Journal of Research of the National Bureau of Standards 1961;A65:297–336.
[3] Mandelkern L, Fatou JG, Howard C. Journal of Physical Chemistry 1964; 68:3386–91.
[4] Point JJ, Rault J, Hoffman JD, Kovacs AJ, Mandelkern L, Wunderlich B, et al. Faraday Discussions 1979;68:365–490.
[5] Armitstead K, Goldbeck-Wood G. Advances in Polymer Science 1992; 100:219–312.
[6] Hoffman JD, Miller RL. Polymer 1997;38:3151–212.
[7] Muthukumar M, Welch P. Polymer 2000;41:8833–7.
[8] Strobl G. European Physical Journal E 2000;3:165–83.
[9] Powers J, Keedy DA, Stein RS. Journal of Chemical Physics 1961;35: 376.
[10] Keller A, Goldbeck-Wood G, Hikosaka M. Faraday Discussion 1993; 109–28.
[11] Olmsted PD, Poon WCK, McLeish TCB, Terrill NJ, Ryan AJ. Physical Review Letters 1998;81:373–6.
[12] Strobl G. European Physical Journal E: Soft Matter 2005;18:295–309.
[13] Strobl G. Progress in Polymer Science 2006;31:398–442.
[14] Heeley EL, Maidens AV, Olmsted PD, Bras W, Dolbnya IP, Fairclough JPA, et al. Macromolecules 2003;36:3656–65.
[15] Ryan AJ, Fairclough JPA, Terrill NJ, Olmstead PD, Poon WCK. Faraday Discussion 1999;13–29.
[16] Imai M, Kaji K, Kanaya T. Physical Review Letters 1993;71:4162–5.
[17] Imai M, Kaji K, Kanaya T, Sakai Y. Physical Review B 1995;52: 12696–704.
[18] Ezquerra TA, LopezCabarcos E, Hsiao BS, BaltaCalleja FJ. Physical Review E 1996;54:989–92.
[19] Terrill NJ, Fairclough PA, Towns-Andrews E, Komanschek BU, Young RJ, Ryan AJ. Polymer 1998;39:2381–5.
[20] Matsuba G, Kaji K, Nishida K, Kanaya T, Imai M. Macromolecules 1999;32:8932–7.
[21] Matsuba G, Kaji K, Nishida K, Kanaya T, Imai M. Polymer Journal 1999;31:722–7.
[22] Katayama K. Sen'i Gakkaishi 1967;23:S300–8.
[23] Katayama K, Amano T, Nakamura K. Kolloid-Zeitschrift and Zeitschrift Fur Polymere 1968;226:125–34.
[24] Yeh GSY, Geil PH. Journal of Macromolecular Science Part B 1967;1: 235–49.
[25] Schultz JM, Lin JS, Hendricks RW, Petermann J, Gohil RM. Journal of Polymer Science Polymer Physics Edition 1981;19:609–20.
[26] Lindenmeyer PH. Polymer Engineering and Science 1974;14:456–63.
[27] Allegra G. Journal of Chemical Physics 1977;66:5453–63.
[28] Akpalu YA, Amis EJ. Journal of Chemical Physics 1999;111:8686–95.
[29] Grasruck M, Strobl G. Macromolecules 2003;36:86–91.
[30] Hoffmann A, Strobl G. Polymer 2003;44:5803–9.
[31] Kawai T, Strobl G. Macromolecules 2004;37:2249–55.
[32] Hobbs JK, Register RA. Macromolecules 2006;39:703–10.
[33] Hafele A, Heck B, Kawai T, Kohn P, Strobl G. European Physical Journal E 2005;16:207–16.
[34] Mirabella FM. Journal of Polymer Science Part B Polymer Physics 2006; 44:2369–88.
[35] Heck B, Kawai T, Strobl G. Polymer 2006;47:5538–43.
[36] Wang H. Polymer 2006;47:4897–900.
[37] Wurm A, Soliman R, Schick C. Polymer 2003;44:7467–76.
[38] Bark M, Zachmann HG, Alamo R, Mandelkern L. Makromolekulare Chemie Macromolecular Chemistry and Physics 1992;193:2363–77.
[39] Hsiao BS, Gardner KH, Wu DQ, Chu B. Polymer 1993;34:3986–95.
[40] Wang ZG, Hsiao BS, Sirota EB, Agarwal P, Srinivas S. Macromolecules 2000;33:978–89.
[41] Kaji K, Nishida K, Kanaya T, Matsuba G, Konishi T, Imai M. Advances in Polymer Science 2005;191:187–240.
[42] Hikosaka M, Watanabe K, Okada K, Yamazaki S. Advances in Polymer Science 2005;191:137–86.
[43] Hobbs JK, Vasilev C, Humphris ADL. Polymer 2005;46:10226–36.
[44] Kavassalis TA, Sundararajan PR. Macromolecules 1993;26:4144–50.
[45] Liu C, Muthukumar M. Journal of Chemical Physics 1998;109:2536–42.
[46] Welch P, Muthukumar M. Physical Review Letters 2001;87:218302/ 218301–4.
[47] Muthukumar M. Philosophical Transactions of the Royal Society of London Series A Mathematical Physical Science and Engineering 2003;361:539–54.
[48] Hu W, Frenkel D. Advances in Polymer Science 2005;191:1–35.
[49] Yamamoto T. Advances in Polymer Science 2005;191:37–85.
[50] Muthukumar M. Advances in Polymer Science 2005;191:241–74.
[51] Gee RH, Lacevic N, Fried LE. Nature Materials 2006;5:39–43.
[52] Chen X, Kumar SK, Ozisik R. Journal of Polymer Science Part B Polymer Physics 2006;44:3453–60.
[53] Heeley EL, Poh CK, Li W, Maidens A, Bras W, Dolbnya IP, et al. Faraday Discussion 2002;122:343–61.
[54] Xiao Z, Ilavsky J, Long GG, Akpalu YA. In: Reiter G, Strobl G, editors. Lecture notes in physics: progress in understanding of polymer crystallization, vol. 714. Berlin Heidelberg: Springer; 2007. p. 117–32.
[55] Li Y, Akpalu YA. Macromolecules 2004;37:7265–77.
[56] Hsiao BS, Gardner KH, Wu DQ, Chu B. Polymer 1993;34:3996–4003.
[57] Akpalu YA, Lin YY. Journal of Polymer Science Part B Polymer Physics 2002;40:2714–27.
[58] Akpalu Y, Kielhorn L, Hsiao BS, Stein RS, Russell TP, van Egmond J, et al. Macromolecules 1999;32:765–70.
[59] Gornick F, Hoffman JD. Industrial and Engineering Chemistry 1966;58: 41–53.
[60] Failla MD, Lucas JC, Mandelkern L. Macromolecules 1994;27:1334–7.
[61] Crist B, Claudio ES. Macromolecules 1999;32:8945–51.
[62] Crist B, Howard PR. Macromolecules 1999;32:3057–67.
[63] Glatter O, Kratky O. Small angle X-ray scattering. New York: Academic Press; 1982.
[64] Segel DJ, Fink AL, Hodgson KO, Doniach S. Biochemistry 1998;37: 12443–51.
[65] Fang XW, Littrell K, Yang X, Henderson SJ, Siefert S, Thiyagarajan P, et al. Biochemistry 2000;39:11107–13.
[66] Crist B. Macromolecules 2006;39:1971–80.
[67] Qian RY. Journal of Macromolecular Science Physics 2001;B40: 1131–51.
[68] Allegra G, Meille SV. Physical Chemistry Chemical Physics 1999;1: 5179–88.
[69] Cahn JW, Hilliard JE. Journal of Chemical Physics 1958;28:258–67.